A composite manipulator utilizing rotary piezoelectric motors: new robotic technologies for Mars *in-situ* planetary science

P. S. Schenker, Y. Bar-Cohen, D. K. Brown, R. A. Lindemann, M. S. Garrett,
E. T. Baumgartner, S. Lee, S.-S. Lih and B. Joffe

Jet Propulsion Laboratory, California Institute of Technology
4800 Oak Grove Drive/MS 125-224
Pasadena, California 91109-8099
paul.s.schenker@jpl.nasa.gov

ABSTRACT

We report a significant advance in space robotics design based on innovation of 3D composite structures and piezoelectric actuation. The essence of this work is development of a new all-composite robotic manipulator utilizing rotary ultrasonic motors (USM). "MarsArmII" is 40% lighter than a prior "MarsArmI" JPL design based in more massive, bulky hybrid metal-composite, joint-link system architecture and DC-motor driven actuation. MarsArmII is a four d.o.f. torso-shoulder-elbow, wrist-pitch robot of over two meters length, weighing four kilograms, and carrying a one kilogram multi-functional science effector with actuated opposable scoops, micro-viewing camera, and active tooling (abrader). MarsArmII construction is composite throughout, with all critical load-bearing joints and effector components being based in a new 3D air layup carbon fiber RTM composite process of our design, and links formed of 2D graphite epoxy. The 3D RTM composite is machinable by traditional metal shop practice, and in early tests such parts bench-marked favorably with aluminum based designs. Each arm link incorporates a surface mounted semiconductor strain gauge, enabling force-referenced closed loop positioning. The principal arm joints are six in-lb rotary USMs acting under optically encoded PID servo control through harmonic drives. We have demonstrated the MarsArmII system for inverse kinematics positioning tasks (utilizing computer vision derived stereo workspace coordinates) that include simulated Martian soil trenching, sample acquisition and instrument transfers, and fresh rock surface exposure by abrasion..

Keywords: robots, actuators, composites, space exploration, sample acquisition

1. INTRODUCTION

If future planetary exploration is to be frequent and cost effective, there must be significant reduction of payload mass, volume, and power. One area of fundamental need is new lightweight, survivable robotic systems for both stationary (landed) and mobile (roving) scientific explorations of Mars [1]. NASA has planned a significant activities of this type within the Mars Surveyor Program. The first such mission, Mars '98/Mars Volatiles and Climate Surveyor (MVACS), will land a robotic arm near the southern polar region, trench and image surrounding icy soils, and conduct an on-site (*in-situ*) chemical analysis of collected samples [2]. Such analyses, along with related meteorological data collection will provide new data on historical and prevailing Martian climate, life, and resources. Subsequent Mars missions, planned for '01, '03, and '05, will likely deploy small instrumented mobile vehicles ("rovers") to survey regions of several kilometers extent, collect and cache rock and soil samples, and transport such samples to an ascent vehicle for earth return and more detailed analysis. Toward these mission objectives, we are carrying out R&D on new integrated robotic concepts and enabling technologies. We previously reported our development of a robotic arm concept [3] that has been selected for Mars'98 flight application. "MarsArmI," as we call that earlier prototype, was 2.3 meter long, three degrees of freedom (d.o.f.) serial manipulator with a single pitch axis d.o.f. scoop for trenching. The arm construction was a hybrid metal-composite architecture -- links were made of 2D graphite epoxy, and the torso/shoulder/roll joints were all metal, utilizing conventional DC-brushed motors. This design was quite novel for its introduction of collapsible telescoping links, whereby the arm could be pneumatically deployed from a stowage volume of about 10 liters. In various instrumented earth laboratory configurations, MarsArmI weighs 9-11 kilograms (and in forthcoming minimal flight realization for the Mars .38 G environment, about 5+ kg). The mechanical design emphasis of our continuing work on robotic arms has been threefold: reduce mass, increase actuation capability from available volume/power, and develop smaller designs (1 kg, .50-.75 m length) suitable to rover as well as lander applications.

To this end we have undertaken a program of new materials and actuator R&D, focus of the first being creation of new lightweight machinable 3D composites (and their system integration with more conventional 2D composites), and the second in innovation of high-torque piezoelectric rotary motors for space applications. Progress on these topics is expected to benefit a wide class of space robot and rover designs, and perhaps be of considerable interest to terrestrial field robotics also. To motivate further discussion we summarize in **Figure 1** some of our related developmental results. While not the topic of this paper, we also are carrying out related R&D on advanced sensors and controls for dexterous, autonomous robotic sampling [4]; this work includes visual and force referenced task-adaptive robotic controls for remotely designated sample selection, pick-up/extraction, and delivery.

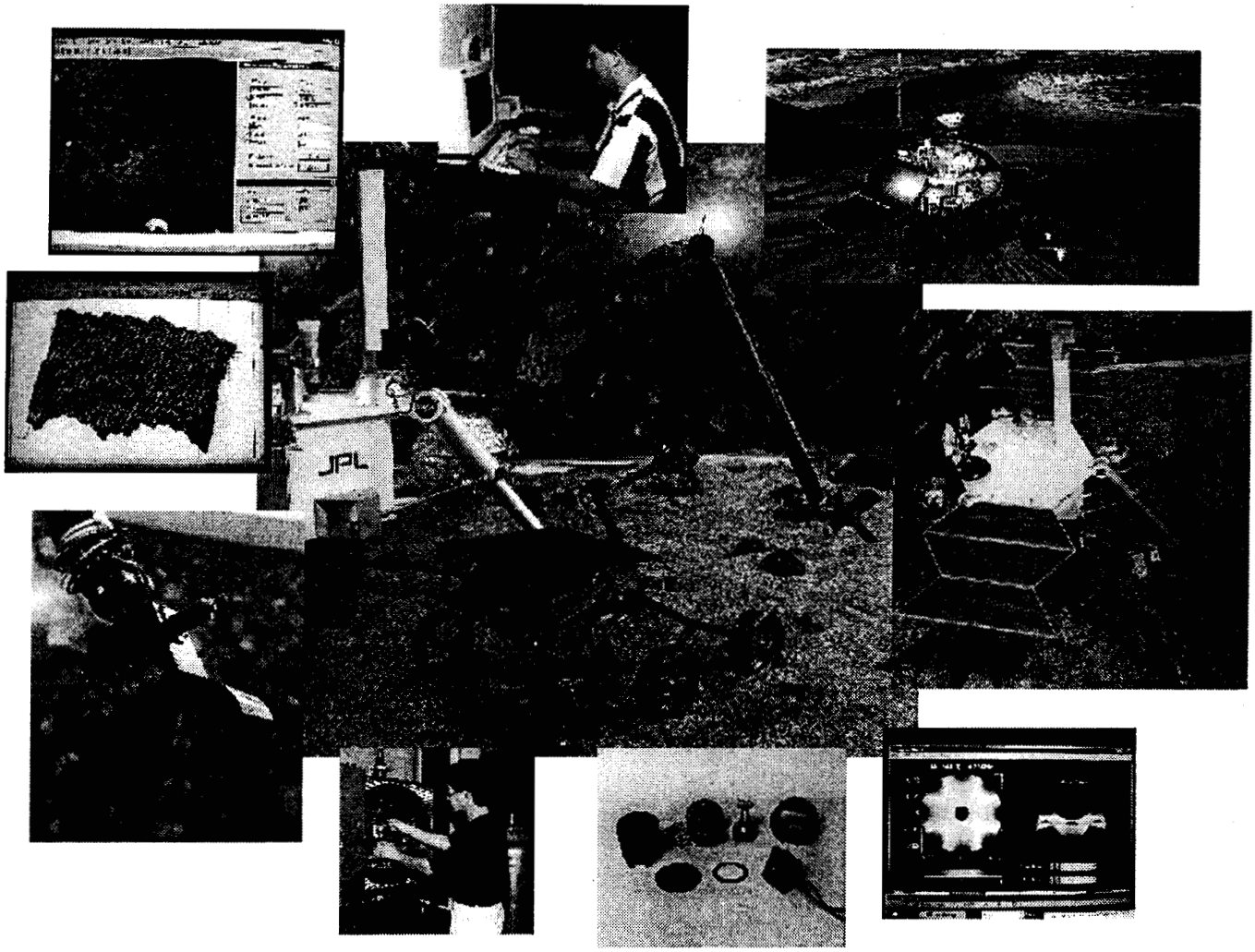

Figure 1. From *upper left, counter-clockwise,* around central figure of the lander-mounted "MarsArmII" of this paper and rover-mounted smaller "MicroArmI (an early developmental model)": A science user interface for visually designating/selecting a particular task action (e.g., "trench along this line & angle, grasp this designated object, locate the arm camera here, etc."). A pseudo-color rendition of the 3-D terrain profile in the arm's workspace, as acquired by lander or rover-mounted stereo cameras. MarsArmII MFSEE ("multi-function science end-effector"). Thermal testing of a low mass, high-torque density rotary ultrasonic actuator for which servo and closed loop inverse kinematics positioning controls were developed. MarsArmII joint assembly showing such an actuator, in conjunction with machined 3D composite parts. Screen display of a finite element modeling tool for analysis and prediction of motor properties, essential to design of the servo controls and drive electronics (models validated in part through electronic speckle pattern interferometry (ESPI) of the modal patterns). "MarsArmI" FY'95 hybrid 2D composite-link/aluminum-joint robot prototype, performing simulated science operations; the MarsArmI concept was selected for NASA's Mars Surveyor '98 science sampling operations, as sketched upper right (ref: *Mars Volatiles and Climate Surveyor*; PI, Professor David A. Paige/UCLA).

2. MarsArmII MECHANICAL ARCHITECTURE

MarsArm II is a second generation lander-based manipulator of the 2 meter, 5 kilogram, 25 watts (earth simulation) class. The design goals are to advance arm design from MarsArmI [3] into 30-40% lighter all composite construction, with an innovative type of ultrasonic motor as the actuator. Inherently the arm is not designed to move quickly; within this constraint, it is still desired to make the arm as stiff as possible to minimize self-deflections and deflection under applied environmental load. The approximate first mode of vibration of the arm, per design parameters below, is estimated at 7 Hz. The maximum self-weight deflection of the arm end-point outstretched on Earth is about .25 inches, while on Mars the deflection would be .10 inches, as accumulates from deflection in the tubes and joints.

MarsArm II, pictured in **Figure 1** above, is a two link all composite serial arm with 4 d.o.f. having a single d.o.f. end-effector with opposable thumb scoop in modified clamshell configuration. The end-effector also carries an integral micro-camera and active abrader, respectively for use in close-geological analysis and powered exposure of fresh rock surfaces (removing oxidized weathering rind). The kinematics arrangement of the arm is a torso-shoulder-elbow-wrist. The torso and shoulder joints connect in series at the base with link 1 connecting to the shoulder joint output. At the end of link 1 the stator side of the elbow joint is connected. At the output or rotor side of the elbow joint is the connection to link 2. The end of link 2 connects to the stator side of the wrist joint, and the rotor side of the wrist joint connects to the end effector housing. The full extent length of MAII is 90 inches (2.3 meters).

MarsArm II is configured as a RRRR robot arm with an additional degree of freedom which is used to open and close the end-effector scoop. The forward kinematics of this arm can be described in standard Denavit-Hartenberg (D-H parameters):

Joint(i)	alpha(i-1)	a(i-1)	d(i)	theta(i)
1	0	0	0	theta(1)
2	-90 deg	a1	d2	theta(2)
3	0	a2	d3	theta(3)
4	0	a3	d4	theta(4)

where a1 = 4 inches, a2 = 44 inches, a3 = 43.895 inches, d2 = 3 inches, d3 = 3 inches, and d4 = 2 inches. Note that the tip position and orientation of the end-effector can also be determined via the forward kinematics through knowledge of the scoop length and the opening angle of the scoop (theta(5)).

The inverse kinematics of MarsArm II have also been determined and are used to compute the joint configuration that achieves a given end-effector position as well as a given in-plane orientation of the end-effector. In general, given the desired end-effector location, the roll joint (theta(1)) is first computed. Once theta(1) is determined, the remainder of the arm can be considered to be a planar arm which maneuvers in what we call the "trenching plane." Then given the end-effector tip position with respect to the trenching plane and the end-effector orientation also with respect to the trenching plane, the last three joint rotations (theta(2) - theta(4)) are calculated. During baseline robotic operations, a stereo camera pair (mounted on the lander base) is calibrated such that they provide an accurate 3D map of the area in front of the lander base (see example of Figure 1 inset, middle left). This 3D map has been determined to be accurate to better than 5 cm. Therefore, given a desired physical space location to approach (selected by the remote operator) and a given end-effector in-plane orientation, the joint configuration which achieves this pose can be determined through the inverse kinematics.

As discussed further below, the arm links are graphite epoxy tubes 40 inches long. The tubes have an outer diameter of 2.5 inches and their wall thickness is 0.040 inches. The graphite epoxy tubes are made of 8 layers of unidirectional fibers in a hand wrapped lay up. The tubes weigh .692 lb apiece. Bonded into the ends of the tubes are reinforcing end caps made of Aluminum 6061-T6 (similar 3D composite parts under evaluation). Each tube has bonded to it near the base a semiconductor force sensor pair used to measure the output torque of the joint for use in force control. The mass of each tube with end caps, and force sensors is 1 lb.

The first three joints of the arm are identical. They utilize a Shinsei (Litton-Westrex, Inc.) USR60S1 ultrasonic motor (USM), that has been experimentally determined to deliver about 4.5 in-lb of torque at stall with an unloaded maximum speed of 100 rpm. The USM's are equipped with a relative optical encoder resolving 500 pulses per shaft revolution. The USMs input to a harmonic drive

having reduction of 160:1. The harmonic drives used are CSF-20-160's provided by Harmonic Systems, Inc. This gives an output stall torque capability for the joints of ~500 in-lb assuming a typical 70% total efficiency. The output side of each joint is held by two Kaydon, Inc. "Really Slim" angular contact bearings with an inner diameter of 2.5 inches. In addition a potentiometer is included internal to the joint as an absolute position device. The potentiometer is a 10 turn rotary coil type. Reduction gearing of the output side of each joint enables the potentiometer to make 4 revolutions for each revolution of the output joint, thus increasing resolution of the potentiometer measurement. These actuation components are structurally integrated within an joint assembly made of a new 3D air layup graphite epoxy machined composite parts, the process for which is further described below. The fully integrated joints, 1-3, cumulatively weigh 2.5 lb.

The end-of-arm wrist joint is a different design, which also serves as basis for the three primary arm joints of the rover-mounted "MicroArm" depicted in Figure 1. The wrist joint utilizes a 1 in-lb Shinsei USR30E3 USM with a no load speed of 300 rpm and an integral optical relative encoder. The 1 in-lb USM inputs to a CSF-14-100 harmonic drive with a reduction of 100:1. The output torque of the wrist joint is approximately 65 in-lb after all of the mechanical losses. The output side of the wrist joint utilizes a single Kaydon "Really Slim" ball bearing with a bore of 1.5 inches. The single bearing is of the x-Type which means it is capable of supporting significant moment loads. The fully assembled wrist joint weighs .7 lb.

Finally, the arm end effector (per lower left inset of Figure 1) also utilizes the 4.5 in-lb Shinsei USM of the MarsArmII primary joints, but with a 10:1 worm screw and two worm gears to power each opposing clamshell digit. The worm gears are mounted on either side of the worm screw. The worm gears are on parallel shafts with a Berg, Inc. ball bearing at the end of each shaft. Given an 80% efficiency of the gearing, the end effector digits share 36 in-lb of torque, powering a 5 inch long scoop and thumb.

The maximum speed of the end effector tip as driven by the torso or shoulder joint is about 5.7 inches/sec, and the lowest speed is .577 inches. The arm is designed to provide a tip force capability of 8 lb., or to carry up to 8 lb. of samples or instrumentation in its end effector. The end effector incorporates a simple grinding (Dremel-style) tool powered by a small DC brushed motor.

3. NEW COMPOSITE MATERIALS FOR ROBOTICS

Mars landed science limitations (mass/volume) can be severe, as imposed by both launch access vehicle capability and science deck volume achievable in the injected payload. Mars'98 is representative: the total science deck integrated payload is budgeted at 20 kilograms, 70 liters, and 25 watts daytime average. This has motivated our development of light, strong materials from which to construct the primary mechanical components of future robots and rovers. In addition to weight savings, the availability of a strong 3D composite, particularly one machinable to precise tolerances like more conventional aluminum or titanium end-fittings it replaces, would afford better differential coefficient of thermal expansion (DCTE) matches to 2D composite struts, tubes, links, etc. Our early progress on this topic, while far from conclusive, is encouraging. We have developed a new 3D air layup resin transfer mold (RTM) process for graphite-resin systems [5] for which the resulting billets are machinable and tappable; we have used early samples to construct MarsArmII, a smaller MicroArm still in integration & test, and perhaps most dramatically, the new "Lightweight Survivable Rover (LSR-1)" prototype pictured in **Figure 2**, next page. As a general rule, we believe it will be possible to realize robotic architectures of 50-70 % conventional (Al) weight, and due to improved DCTE properties, achieve more robust mechanical behavior at interfaces subject to repeated thermal stress loads induced by diurnal planetary cycling. The latter is important given future plans for Mars and other planetary surface missions of many months extent. Herein, we briefly outline the 2D composite tube and 3D composite part processes used in MarsArmII, with emphasis on the 3D work.

3.1 2D Composites

Methods for the fabrication of composite tubing and tooled parts from unidirectional tape are generally well developed. In the case of the tubes for MarsArmI, an AS-4/3501-6 (AS-4 carbon fiber and 3501-6 epoxy) pre-impregnation system was selected. This system was chosen because behavior of the 3501-6 resin is well understood, and the "pre-preg" system is readily available. A second system, AS-4/RS-3, was chosen for purposes of comparative evaluation. The RS-3 resin system is a polycyanate, and polycyanates are known for their superior resistance to moisture uptake, radiation, and micro-cracking at cryogenic temperatures. The primary goal in evaluating the RS-3 system was to compare the mechanical properties of the RS-3 and 3501-6 pre-pregs at room and cryogenic temperatures, and to develop a cure cycle for tubes made with RS-3 pre-preg using the trapped mandrel technique.

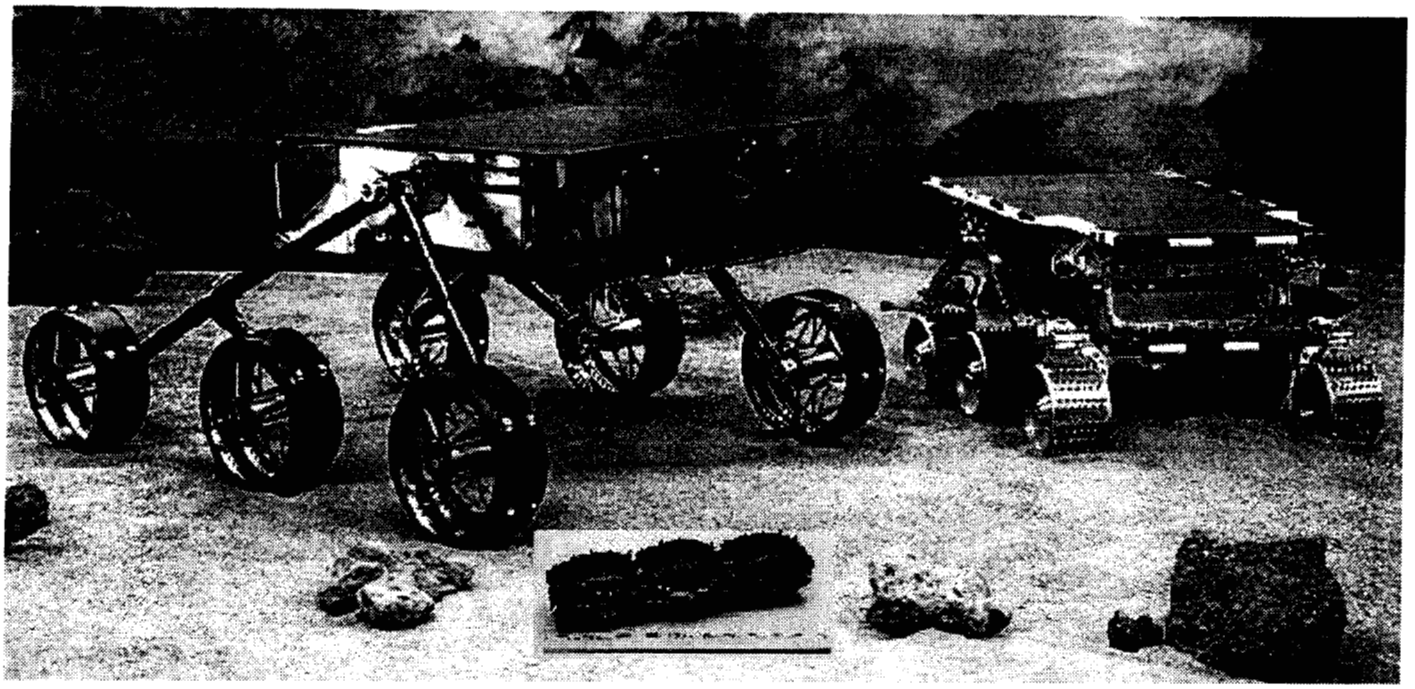

Figure 2. Lightweight Survivable Rover, LSR-1 (left): a 7 kilogram (Kg) rover R&D prototype having 20 centimeter (cm) diameter wheels, 97 cm length, 70 cm width, and 29 cm ground clearance (note: LSR-1 is shown prior to bonding of composite helical growsers to wheel rims). Sojourner (right): the recently launched 11+ Kg '96 Mars Pathfinder microrover flight experiment (13 cm wheels, 63 cm length, 45 cm width, and 15 cm ground clearance). LSR-1, which incorporates significant advances in composite and thermal materials, as well as a new exoskeletal thermal-structural chassis, is conceived to operate over larger obstacles (~.4 meters), broader thermal latitudes (equatorial to near polar regions), longer distances (multiple kilometers), and extended duration (multiple months). LSR-1 introduces a novel spot pushbroom sensor, enabling the rapid detection-and-avoidance of hazards in variably featured terrain, while using less power and computation. A central element of LSR design is "Volume Efficient Mobility," wherein wheels and mobility running gear collapse for transport, thus allowing rover stowage during flight to as little as 25% operational field volume. The LSR mobility platform concept scales to larger/heavier vehicles, and is being used for a new JPL 40+ Kg class long range mobile science design.

Testing of both the AS-4/3501-6 and the AS-4/RS-3 materials was performed using flat plates. The plates were fabricated using the same layup as the tubes, and autoclave cured at the same pressure the trapped mandrel was designed to produce (50 PSI). The tests to be cumulatively performed on the panels include axial tension, four point flexure, and a specially designed "true shear" inter-laminar shear test. Additionally, the tensile and flexural tests are to be repeated at -100 °C in order to evaluate the differences in the performance of the two matrix resins (epoxy and polycyanate). Finally, some small diameter tubes of both materials will be tested in tension to validate the accuracy of the flat panel tests. Some summary test results are tabulated in **Figure 3**, next page.

The design of the tubes was based on the primary loading that they would see in service, as well as the need to keep them as light as possible. The primary service loads on the tubes are in axial bending, with some minimal secondary torsional loading due to the offset of the tubes at the joint. The layup thus selected was [0/0/+30/0/0/-30/0/0]. This layup kept the wall thickness to 0.040" to minimize weight, and maximized the number of axial plies to provide the required axial strength and stiffness. The 30 degree plies were included to provide a degree of torsional strength, as well as crush resistance. Normally, an additional set of +30 and -30 plies would be included to balance the layup and prevent distortion of the tubes, but the requirement for maximum axial stiffness required that those plies not be included. The only distortion seen in the tubes was seen in the large (2.5") diameter tubes, and this was within tolerable limits. Based on the layup, the predicted strength of the tubes is 230 KSI, and the predicted modulus (using the HAVOC laminate analysis code) is 17 MSI. Given the above strength estimate, the large tubes should have a breaking strength of 72,250 lb., and the small (1.25" diameter) tubes should have a strength of 36,100 lb.

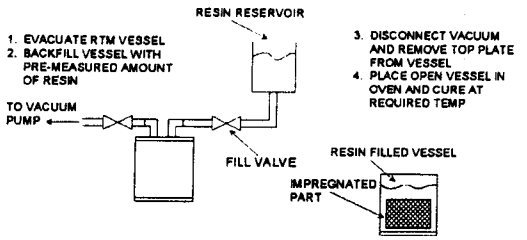

Resin Transfer Mold (RTM) Process

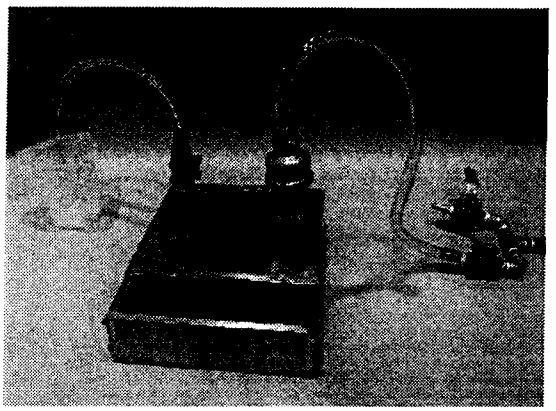

MATERIAL	TENSION	4 POINT FLEXURAL	COLD TENSION	COLD FLEXURAL
AS4/3501-6	2D graphite-epoxy pre-preg			
STRENGTH (KSI)	213.0	223.1	217.2	279.9
MODULUS (MSI)	17.0	17.6	17.3	18.0
AS4/RS-3	2D graphite-polycyanate pre-preg system			
STRENGTH (KSI)	206.1	200.2	258.0	273.0
MODULUS (MSI)	17.2	17.4	17.8	17.5
AL-C 3D	3D lower density carbon fiber post-preg system			
"X" OR "Y" DIR				
STRENGTH (KSI)	5.8	11.2	NA	NA
MODULUS (MSI)	0.8	0.8	NA	NA
"Z" DIR, NO BL				
STRENGTH (KSI)	7.0	NA	NA	NA
MODULUS (MSI)	1.2	NA	NA	NA
"Z" DIR, ACROSS BL				
STRENGTH (KSI)	5.8	12.8	NA	NA
MODULUS (MSI)	1.2	1.2	NA	NA
SPC 3D	3D higher density carbon fiber post-preg system			
"X" OR "Y" DIR				
STRENGTH (KSI)	NA	22.5	NA	NA
MODULUS (MSI)	NA	1.7	NA	NA

Figure 3. RTM apparata for 3D composite billet processing and tabulated results of 2D and 3D composite tests

3.2 3D Composites

Most composites (with the exception of 3D carbon/carbon components) are 1D or 2D layups. Mechanical joints of a structure like MarsArmII carry complex, triaxial loads, while most composites can carry only selective uniaxial or biaxial laods. The seeming solution is to use a more isotropic 3D preform. Unfortunately, conventional 3D preforms are braided, polar woven, or block (orthogonal) woven. These types of architectures tend to be somewhat coarse, and when impregnated with resin have large matrix (or resin) pockets. These matrix pockets result in weak points, particularly when the material is machined into small cross sections, as is our desire. We have thus begun development of a class of newer materials, umimpregnated preforms of which were sourced from BF Goodrich Aerospace (BFG) – non-woven, random air layup carbon 3D fibers. We have so far evaluated two such systems (designated AL-C and SPC) which once processed per the general procedure below, have bulk densities about half that of Al. The materials differ markedly in fiber density, with predictable resulting differences in their tested mechanical properties.

[*vacuum/atmospheric pressure RTM process, Figure 3 above*]:

1. Place dry preform into impregnation vessel and evacuate. Hold vacuum for 2 hours.
2. Attach resin reservoir to inlet valve. Open valve until resin has been transferred from reservoir (sufficient to cover preform). Hold under vacuum for a further 2 hours.
3. Release vacuum and remove top cover from impregnation vessel, verify that preform is fully submerged. Place vessel in oven.
4. Cure preform by heating to 210 °F for 2 hours, this allows resin flow and helps to fill any remaining voids. Raise temperature to 250 °F and hold for four hours; this fully cures the resin.
5. Remove cured billets from vessel. The cured material may then be machined using conventional methods, except that diamond abrasive blades should be used for sawing. Machining should be done with carbide tools, as this material is very abrasive.

The final part is obtained from step 5 above. Experiments were also made in producing threaded holes. This was found to be feasible using conventional taps from 2-56 up to 1/4"-20. Thread shear tests were performed on threads from #2 up to #8. The thread shear strength for the 2-56 threads varied from 44 KSI to 90 KSI, for 4-40 and up, the thread shear strengths were around 78 KSI. This indicates that the #2 thread is small enough that it is below the level for which this material homogeneous, and that the true thread shear is approximately 78 KSI. It should also be noted that the true shear strength is not the same as thread shear. Thread shear should only be used in determining the amount of load that can be put on a screw without pulling it out of the hole.

Our evaluation of the AL-C, the only material available in bulk for the initial MarsArmII fabrication, suggests significant improvements in bulk mechanical properties will be obtained through use of SPC or other higher density preforms as they become available. The first indication was a large amount of micro-cracking observed in early RTM process runs of AL-C. It was ultimately determined that such micro-cracking was the result of coefficient of thermal expansion mismatch between the matrix resin and the fiber preform, and that the cracking occurred as the material cooled from the 350 °F cure temperature down to room temperature. This problem was mostly resolved by changing the resin/catalyst formulation to allow for a 250 °F cure. It is clear that AL-C, as processed, would be unsuitable for use in the -100 °C environment on Mars. We also observed that the post-process AL-C material has some occurrence of "cells", as are seen in woven 3D materials; this was not seen in the SPC material. The lower fiber volume also resulted in a predictably lower density than the SPC, at 1.2 g/cc, and in a markedly lower strength, of 11.5 KSI. Early indications, as observed during our continued development of SPC material and a new small arm robotic prototype based on it, is that these structural concerns and low temperature (thermal cycling) limitations will be resolved.

4. ROBOT ACTUATION BY ROTARY PIEZOELECTRIC MOTORS

MarsArmII introduces use of rotary ultrasonic motors (USMs) for precision robotic actuation. Such motors, initially developed in Japan and Europe for small consumer electronic/appliance applications, have potentially advantageous properties for space robotics if they can be scaled to higher power outputs, cryo-vacuum environments, and be demonstrated for well-regulated position and force control. Desirable USM features include high torque density (x3-10 that of DC motors), inherently low operating speeds, reduced gearing complexity/mass, high holding torque, self-braking (non-backdriveable), simple mechanical construction, and annular stator-rotor geometry (allowing pass-through of optics/instrumentation/etc.). While the principles of USM operation are well understood and a number of basic designs have been demonstrated [6], this class of motors and its modeling is far from optimized in either design or materials. The basic USM operational concept is illustrated below in **Figure 4**:

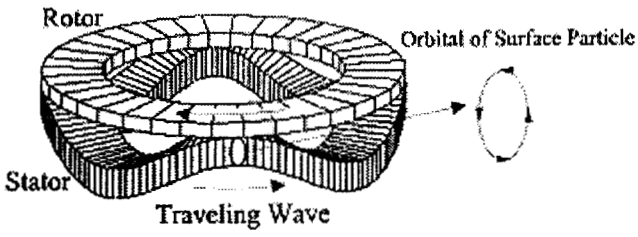

Figure 4. Rotary ultrasonic motors excite their gross mechanical motion through piezoelectric transduction of flexural deformations onto the stator (e.g., an alternating poled ferroelectric). When driven at a resonant frequency, the stator sustains a traveling wave whose elliptic orbital particle motions can be frictively impressed on a rotor which counter-propagates. Design of the USM rotor-stator interface is key to actuation efficiency, and issues include contact pattern, material wear, maintaining uniform contact force, and potential delamination due to DCTE effects.

We have been working along several fronts to advance USM technology for space robot and rover applications [7]. This R&D effort includes: 1) finite element models for motor simulation and parametric trades analysis; 2) new stator designs delivering higher transduction efficiency/power in given volume, and 3) mechanization interfaces robust to low temperatures and repeated thermal cycling (viz. -20 to -100 °C Mars ambients), and 4) experimental characterization of motor behavior at lower temperatures. The modeling effort is important, given a current lack of simulation tools incorporating parametric details of the rotor-stator interface, piezoelectric material coefficients, stator geometry, etc. Lih and Bar-Cohen address this modeling development in a companion paper [8]. Early results are encouraging; theoretical predictions and experimental measurements of USM modal response, resonance frequency, and other operating characteristics are in excellent agreement (as confirmed through dynamic observations of wave modes by electronic speckle pattern interferometry). To our knowledge there has been little if any prior experimentation on low temperature operation of USMs. To establish a baseline, and prepare for experimental analysis for new motors under construction, we have developed the cryogenic environmental test facility shown in **Figure 5** on next page. This

instrumented SATEC, Inc., chamber, capable of 120 °K and 20 mTorr, incorporates a computer controlled brake and load cell for the collection of motor torque-speed characteristics, time-torque transients and other salient motor steady state and dynamic data. Figure 5 shows preparation of a cryo-vac experiment, the instrumented testbed and torque-speed curves obtained for a commercial USM (Shinsei USR30E3) as utilized in the MarsArmII wrist joint and also t/s/e joints of the smaller MicroArm (Figure 1):

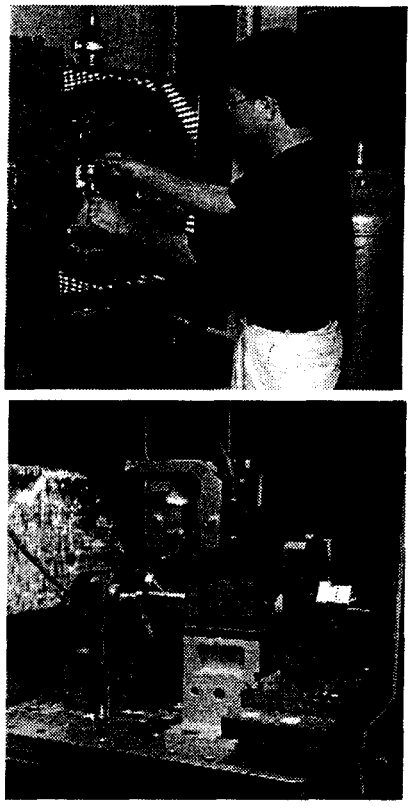

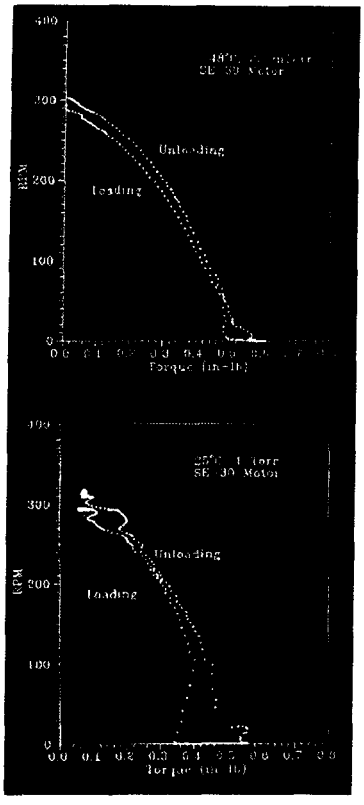

Evaluation of commercial rotary USM for cryo-vacuum torque speed characteristics (top, -48 °C/20mTorr, bottom 25 °C/1 ATM)

- Shinsei USR30E3, nominal 1 in-lb
- MarsArmII wrist (and MicroArmI)
- specified by Mfr , for > -10 °C use
- operated to seizure at close to -50 °C
- low-T testing at 20mTorr, inert ATM
- no hysteresis on recycling
- no coronal effects noted
- no vacuum welding noted

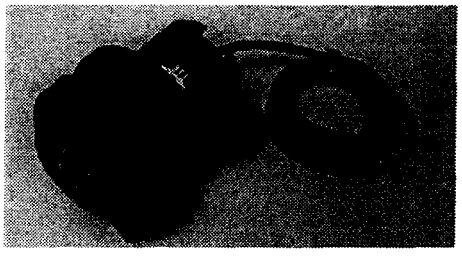

Figure 5. Cryo-vac experiment in preparation (S-S. Lih) for collection of rotary ultrasonic motor data; torque-speed data collected for commercial motor at room and low temperatures, and typical 3D composite joint assembly utilizing this motor

The results of these initial low temperature tests are somewhat surprising, and are a positive indicator for further development of low-temperature optimized USM designs. The test device is nominally specified for room temperature and 1 ATM operation, not to be used below -10 °C. However, we observed repeatable operations to ~ -50 °C, with seizure seemingly induced by DCTE tolerance effects on the stator-rotor interface (The underlying piezoelectric transduction ideally extends to near 0 °K). Further, there appeared to be no vacuum induced degradation such as coronal discharge, welding, etc.

Our most recent USM research addresses development of new stator designs that will be more tolerant of low temperature and capable of higher transduction efficiency. Bar-Cohen et al. have introduced the "reverse segmented and stacked [9]" stator, a design facilitating low cost batch manufacture, and forgiving of temperature induced expansion/contraction effects. In this USM, the stator transducer elements (cf. Figure 4.) are assembled as individual, contiguous pie-segments on the supporting base, with adjacent elements having alternating polarity and being driven in phase quadrature. This effectively implements the alternate poling of a conventional continuous stator while obviating some labor-intensive, high temperature, high-voltage spatial repoling processes and associated intermediate electrode depositions. Temperature induced stress effects are essentially localized to the segments versus propagating over the entire stator geometry. Further, the segmented elements can in principle be stacked vertically to excite high particle excursions at relatively drive low voltages. We have completed a first such reverse segmented motor prototype of comparable size to the Shinsei commercial motor above. In initial room temperature operations the two motors exhibit comparable torque-speed curves, and we are now beginning low temperature tests.

ACKNOWLEDGEMENTS

This work was carried out at the Jet Propulsion Laboratory, California Institute of Technology, under a contract with the National Aeronautics and Space Administration. We gratefully acknowledge support of the NASA Telerobotics Program for this research.

REFERENCES

1. C. R. Weisbin, D. Lavery, and G. Rodriguez, "Robotics technology for planetary missions into the 21st century," in Proc. 1997 Intl. Conf. Mobile Planetary Robots and Rover Roundup, Santa Monica, CA, January (Interplanetary Society, L. Friedman).
2. D. A. Paige, et al., "Mars Volatiles and Climate Surveyor (MVACS) – Integrated Payload Proposal for the Mars Surveyor Program '98 Lander (Volume 1: Investigation and Technical Plan)," Response to NASA A0 No. 95-OSS-3, University of California, Los Angeles, August, 1995. See also *http://mvacs.ess.ucla.edu.*
3. P. S. Schenker, D. L. Blaney, D. K. Brown, Y. Bar-Cohen, S-S. Lih, R. A. Lindemann, E. D. Paljug, J. T. Slostad, G. K. Tharp, C. E. Tucker, C. J. Voorhees, and C. Weisbin, Jet Propulsion Lab.; E. T. Baumgartner, Mich. Tech. Univ.; R. B. Singer, R. Reid, Univ. of Arizona, "Mars lander robotics and machine vision capabilities for *in situ* planetary science," in Intelligent Robots and Computer Vision XIV, SPIE Proc. 2588, Philadelphia, PA, October, 1995; see also, E. T. Baumgartner and P. S. Schenker, "Autonomous image-plane robot control for Martian lander operations," in Proc. 1996 IEEE Intl. Conf. Robotics and Automation , pp. 726-731, Minneapolis, MN, April; E. T. Baumgartner and N. A. Klymyshyn, "A sensitivity analysis for a remote vision-guided robot arm under imprecise supervisory control," in Sensor Fusion and Distributed Robotic Agents, Proc. SPIE 2905, Boston, MA, November, 1996.
4. S. Lee and P. Schenker, "Autonomous synthesis of goal-oriented behaviors for intelligent robotic systems," in IROS '96 workshop on "Event-Driven Sensing, Planning and Control for Robotic Systems." Osaka, Japan, Nov. 1996. (edited text, Springer-Verlag); S. Lee and P. Schenker, "Sensor fusion and planning with perception and action network," in Proc. IEEE/SICE/RSJ Multi-sensor Fusion and Integration for Intelligent Systems (MFI'96), Washington, DC., December, 1996; and S. Lee, S-C. Ahn, A. Meyyappan, and P. Schenker, "3D sensing with hand-eye camera," in Sensor Fusion and Distributed Robotic Agents, Proc. SPIE 2905, Boston, MA, November, 1996.
5. D. K. Brown, "Near isotropic, machinable, resin transfer molded composite," Disclosure of New Technology, Docket 19918, Jet Propulsion Laboratory, Pasadena, CA, March, 1996.
6. T. Ueha and Y. Tomikawa, *Ultrasonic Motors - Theory and Applications*, Oxford Science Publications, Oxford, England, 1993; see also, J. Hollerbach, I. W. Hunter, and J. Ballantyne, "A comparative analysis of actuator technologies for robotics," in *Robotics Review 2 (eds. O. Khatib, J. Craig, and T. Lozano-Perez)*, The MIT Press, Cambridge, MA, 1992.
7. Y. Bar-Cohen, S.-S. Lih and N. W. Hagood, "Miniature ultrasonic rotary motors", 2nd Micromachining Workshop, American Vacuum Society, Anaheim, CA, September, 1995.
8. S-S. Lih and Y. Bar-Cohen "Rotary piezoelectric motors actuated by traveling waves," in Enabling Technologies: Smart Structures and Integrated Systems, SPIE Proc. 3041, San Diego, CA, March 1997.
9. Y. Bar-Cohen, S.-S. Lih and W. Grandia, "High torque ultrasonic motor system using a series of connected individual motors and a stack of piezoelectric drivers," Disclosure of New Technology, Docket 19835, Jet Propulsion Laboratory, Pasadena, CA, November, 1995 (Patent Pending)